JOURNAL OF GUIDANCE, CONTROL, AND DYNAMICS
Vol. 29, No. 2, March–April 2006

Engineering Notes

ENGINEERING NOTES are short manuscripts describing new developments or important results of a preliminary nature. These Notes should not exceed 2500 words (where a figure or table counts as 200 words). Following informal review by the Editors, they may be published within a few months of the date of receipt. Style requirements are the same as for regular contributions (see inside back cover).

Robust Rendezvous Navigation in Elliptical Orbit

Christopher D. Karlgaard*
Analytical Mechanics Associates, Inc., Hampton, Virginia 23666

Introduction

THE autonomous rendezvous and docking of spacecraft in orbit has been identified as a key development area for future space programs.[1] Several scenarios have been outlined that require autonomous rendezvous and docking capabilities, such as robotic sample return missions,[2] in-space assembly of modular systems,[3] and the rendezvous of crewed Mars landers to an Earth-return vehicle.[1]

Autonomous rendezvous and docking scenarios will most likely involve the use of radar for relative navigation at some stage in the process. In low Earth orbit (LEO), the system may rely on global positioning system measurements until the spacecraft are in close proximity, then switch to a radar or laser sensing system. Rendezvous scenarios away from LEO, perhaps in lunar orbit, for example, will likely rely on radar or laser measurements for the majority of the relative sensing capability.

The processing of the relative sensor measurements to determine the maneuver spacecraft position and velocity relative to the target spacecraft can be accomplished by one of several means. Perhaps the most widely used technique in this area of application is the Kalman filter.[4] The Kalman filter is a recursive weighted least-squares or minimum ℓ_2 norm (sample mean) estimation procedure and is a maximum likelihood technique assuming that the error statistics follow Gaussian probability distributions.

Unfortunately, the least-squares method is not a robust estimation technique. That is, the estimation technique fails to perform adequately when the true error statistics follow non-Gaussian probability distributions, particularly those with much thicker tails than the Gaussian distribution.[5,6] Because radar systems are known to exhibit non-Gaussian random measurement errors,[7] and because orbital state error predictions are known to be non-Gaussian in nature,[8] it is important to develop estimation techniques for radar-based rendezvous navigation that are robust with respect to deviations from the assumption of Gaussianity.

One such technique is the Huber filter,[9,10] which is a combined minimum ℓ_1 and ℓ_2 norm estimator. The minimum ℓ_1 norm estimator (sample median) is a maximum-likelihood estimator with the assumption that the error statistics follow the Laplacian distribution. The Huber estimator is a blend of the two estimators that seeks to use the best of both techniques, in particular, the robustness of the sample median and the efficiency of the sample mean. It is the purpose of this Note to apply the Huber filter to the problem of radar or laser-based rendezvous navigation.

Received 26 July 2005; revision received 19 September 2005; accepted for publication 20 September 2005.

*Project Engineer, Analytical Mechanics Associates, Inc., 303 Butler Farm Road, Suite 104A; karlgaard@ama-inc.com. Senior Member AIAA.

Review of the Estimation Technique

This section concerns the problem of estimating the state of the system of ordinary differential equations

$$\dot{\boldsymbol{x}} = \boldsymbol{f}(\boldsymbol{x}, \boldsymbol{u}, \boldsymbol{v}, t) \tag{1}$$

where $\boldsymbol{x}$ is the state vector, $\boldsymbol{u}$ are the deterministic inputs to the system, and $\boldsymbol{v}$ are random inputs to the system. The mean value of $\boldsymbol{v}$ is $\bar{\boldsymbol{v}} = \boldsymbol{0}$, and its covariance is $\boldsymbol{Q}$. It is assumed that the state of the system can be measured at discrete times in the form of a linear model given as

$$\boldsymbol{y}_k = \boldsymbol{H}_k \boldsymbol{x}_k + \boldsymbol{w}_k \tag{2}$$

where the subscript k refers to the value of the parameter at time t_k, $\boldsymbol{y}_k$ is the measurement at time t_k, and $\boldsymbol{w}_k$ is the measurement noise at time t_k. The mean value of $\boldsymbol{w}_k$ is $\bar{\boldsymbol{w}}_k = \boldsymbol{0}$, and its covariance is $\boldsymbol{R}_k$.

The Huber filter is a technique for estimating the state of systems of differential equations described in the form provided in Eqs. (1) and (2). The filter is a predictor–corrector approach in which the state predictions are computed by numerical integration of the dynamic model, and state corrections are obtained by a weighted linear combination of the predicted measurements and the actual measurements. In this approach, the state and covariance predictions are given as

$$\bar{\boldsymbol{x}}_k = \hat{\boldsymbol{x}}_{k-1} + \int_{t_{k-1}}^{t_k} \boldsymbol{f}[\bar{\boldsymbol{x}}(t), \boldsymbol{u}, \bar{\boldsymbol{v}}, t]\, \mathrm{d}t \tag{3}$$

$$\bar{\boldsymbol{P}}_k = \hat{\boldsymbol{P}}_{k-1} + \int_{t_{k-1}}^{t_k} \{\boldsymbol{A}[\bar{\boldsymbol{x}}(t), t]\bar{\boldsymbol{P}}(t) + \bar{\boldsymbol{P}}(t)^T \boldsymbol{A}[\bar{\boldsymbol{x}}(t), t]^T + \boldsymbol{B}[\bar{\boldsymbol{x}}(t), t]\boldsymbol{Q}(t)\boldsymbol{B}[\bar{\boldsymbol{x}}(t), t]^T\}\, \mathrm{d}t \tag{4}$$

where $\bar{\boldsymbol{x}}_k$ is the predicted value of the state at time t_k, based on the propagation of estimated value of the state at time t_{k-1}, which is $\hat{\boldsymbol{x}}_{k-1}$. Similarly, $\bar{\boldsymbol{P}}_k$ is the predicted state error covariance matrix at time t_k, and $\hat{\boldsymbol{P}}_{k-1}$ is the estimated state error covariance matrix and time t_{k-1}. Also, the matrices $\boldsymbol{A}$ and $\boldsymbol{B}$ are given by

$$\boldsymbol{A}(t) = \left.\frac{\partial \boldsymbol{f}}{\partial \boldsymbol{x}}\right|_{x=\bar{x}(t), v=\bar{v}} \tag{5}$$

$$\boldsymbol{B}(t) = \left.\frac{\partial \boldsymbol{f}}{\partial \boldsymbol{v}}\right|_{x=\bar{x}(t), v=\bar{v}} \tag{6}$$

The state correction obtained at the time of the measurement update takes the form of a linear regression problem between the predicted state and the observed quantity.[11] If the true value of the state is written as $\boldsymbol{x}_k$ and the state prediction error is written as $\boldsymbol{\delta}_k = \boldsymbol{x}_k - \bar{\boldsymbol{x}}_k$, then the state prediction may be expressed as $\bar{\boldsymbol{x}}_k = \boldsymbol{x}_k - \boldsymbol{\delta}_k$. The linear regression problem then takes the form

$$\begin{Bmatrix} \boldsymbol{y}_k \\ \bar{\boldsymbol{x}}_k \end{Bmatrix} = \begin{bmatrix} \boldsymbol{H}_k \\ \boldsymbol{I} \end{bmatrix} \boldsymbol{x}_k + \begin{Bmatrix} \boldsymbol{w}_k \\ -\boldsymbol{\delta}_k \end{Bmatrix} \tag{7}$$

By definition of the quantities

$$\boldsymbol{T}_k = \begin{bmatrix} \boldsymbol{R}_k & \boldsymbol{0} \\ \boldsymbol{0} & \bar{\boldsymbol{P}}_k \end{bmatrix} \tag{8}$$

$$\boldsymbol{z}_k = \boldsymbol{T}_k^{-\frac{1}{2}} \begin{Bmatrix} \boldsymbol{y}_k \\ \bar{\boldsymbol{x}}_k \end{Bmatrix} \tag{9}$$

$$\boldsymbol{G}_k = \boldsymbol{T}_k^{-\frac{1}{2}} \begin{bmatrix} \boldsymbol{H}_k \\ \boldsymbol{I} \end{bmatrix} \tag{10}$$

$$\boldsymbol{\xi}_k = \boldsymbol{T}_k^{-\frac{1}{2}} \begin{Bmatrix} \boldsymbol{w}_k \\ -\boldsymbol{\delta}_k \end{Bmatrix} \tag{11}$$

the linear regression problem is transformed to

$$\boldsymbol{z}_k = \boldsymbol{G}_k \boldsymbol{x}_k + \boldsymbol{\xi}_k \tag{12}$$

In this transformed regression problem, the covariance of $\boldsymbol{\xi}_k$ is simply the identity matrix, as can be seen from expanding the expectation $E(\boldsymbol{\xi}_k \boldsymbol{\xi}_k^T)$.

The Huber filter measurement update arises from the minimization of the cost function

$$\beta(\boldsymbol{x}_k) = \sum_{i=1}^{n} \lambda(\zeta_i) \tag{13}$$

where ζ_i refers to the ith component of the normalized residual vector, $\zeta_i = (\boldsymbol{G}_k \boldsymbol{x}_k - \boldsymbol{z}_k)_i$, and the function λ is known as the "score function," defined as

$$\lambda(\zeta_i) = \begin{cases} \frac{1}{2}\zeta_i^2 & \text{for } |\zeta_i| < \gamma \\ \gamma|\zeta_i| - \frac{1}{2}\gamma^2 & \text{for } |\zeta_i| \geq \gamma \end{cases} \tag{14}$$

where γ is a tuning parameter.

The solution of the Huber regression problem is determined from the derivative of the cost function

$$\sum_{i=1}^{n} \psi(\zeta_i)\zeta_i = 0 \tag{15}$$

where $\psi(\zeta_i) = \lambda'(\zeta_i)/\zeta_i$ is given as

$$\lambda(\zeta_i) = \begin{cases} 1 & \text{for } |\zeta_i| < \gamma \\ \gamma/|\zeta_i| & \text{for } |\zeta_i| \geq \gamma \end{cases} \tag{16}$$

The solution of Eq. (15) is typically achieved in one of two ways: a Newton–Raphson iteration, or the iteratively reweighted algorithm, which is commonly attributed to Beaton and Tukey.[12] In this Note, the latter method will be used. The algorithm may be derived as follows. First, by the definition of the matrix $\Psi = \text{diag}\,[\psi(\zeta_i)]$, Eq. (15) may be rewritten as

$$\boldsymbol{G}_k^T \Psi (\boldsymbol{G}_k \boldsymbol{x}_k - \boldsymbol{z}_k) = \boldsymbol{0} \tag{17}$$

Equation (17) may be expanded to yield $\boldsymbol{G}_k^T \Psi \boldsymbol{G}_k \boldsymbol{x}_k = \boldsymbol{G}_k^T \Psi \boldsymbol{z}_k$, which may be solved for $\boldsymbol{x}_k$ to give $\boldsymbol{x}_k = (\boldsymbol{G}_k^T \Psi \boldsymbol{G}_k)^{-1} \boldsymbol{G}_k^T \Psi \boldsymbol{z}_k$. When it is noted that the matrix Ψ depends on the residuals ζ_i, and hence on $\boldsymbol{x}_k$, the following iterative solution to Eq. (17) is expressed as

$$\boldsymbol{x}_k^{(j+1)} = (\boldsymbol{G}_k^T \Psi^{(j)} \boldsymbol{G}_k)^{-1} \boldsymbol{G}_k^T \Psi^{(j)} \boldsymbol{z}_k \tag{18}$$

where the superscript (j) refers to the iteration index. The method can be initialized by using the least-squares solution $\boldsymbol{x}_k^{(0)} = (\boldsymbol{G}_k^T \boldsymbol{G}_k)^{-1} \boldsymbol{G}_k^T \boldsymbol{z}_k$. The converged value from the iterative procedure is taken as the corrected state estimate following a measurement update $\hat{\boldsymbol{x}}_k$.

Finally, the state estimate error covariance matrix is computed from

$$\hat{\boldsymbol{P}}_k = (\boldsymbol{G}_k^T \Psi \boldsymbol{G}_k)^{-1} \tag{19}$$

using the final value of Ψ corresponding to the converged state estimate.

Note that as $\gamma \to \infty$, the Huber filtering problem reduces to the least-squares estimator (Kalman filter or sample mean). Specifically, when $\gamma \to \infty$, the matrix $\Psi \to \boldsymbol{I}$, and Eq. (17) may be solved exactly in one iteration step and is equal to the Kalman filter solution. Also note that as $\gamma \to 0$, the problem reduces to the least absolute value estimator (sample median). This blend of estimation techniques gives the Huber estimator a robustness against deviations from Gaussian distributed random measurement errors, at the cost of only a slight loss of efficiency in estimation when the errors do follow the Gaussian distribution and an increase in computational effort due to the iterative technique required for the measurement update step. This robustness arises from the Ψ matrix and that all residuals are not weighted equally. In particular, large residuals are down-weighted in the iterative solution technique by the inverse of the magnitude of the residual.[13,14]

The specific value of γ used is typically taken to be $\gamma = 1.345$ to give 95% asymptotic efficiency for estimation problems with Gaussian distributed random errors. In other words, the Huber filter with this choice of γ will lead to estimation error variances that are 5% larger than that of the Kalman filter when the measurement error statistics are truly Gaussian. References 9 and 15 contain additional information on the tuning of the parameter γ.

The next section describes the application of both the Kalman filter and the Huber filter to the problem of spacecraft navigation during rendezvous maneuvers, using range and line of sight measurements.

Application to Spacecraft Rendezvous Navigation

In this section, the application of the robust estimation technique to an example spacecraft rendezvous navigation problem is discussed. The mechanics of the relative motion are developed first, followed by the development of a simple guidance scheme for the purposes of simulating the motion of the vehicle during the rendezvous maneuver. Both the Kalman filter and the Huber filter are applied to estimate the relative position and velocity of the spacecraft along the rendezvous trajectory in a numerical simulation.

Rendezvous Dynamics and Measurement Equations

The equations of motion for a spacecraft relative to another spacecraft in an elliptical Keplerian orbit can be expressed by the system of differential equations (see Ref. 16):

$$\ddot{x} = 2\omega\dot{y} + \dot{\omega}y + \omega^2 x + \frac{\mu}{r^2} - \frac{\mu(r+x)}{[(r+x)^2 + y^2 + z^2]^{\frac{3}{2}}} + u_x + v_x \tag{20}$$

$$\ddot{y} = -2\omega\dot{x} - \dot{\omega}x + \omega^2 y - \frac{\mu y}{[(r+x)^2 + y^2 + z^2]^{\frac{3}{2}}} + u_y + v_y \tag{21}$$

$$\ddot{z} = -\frac{\mu z}{[(r+x)^2 + y^2 + z^2]^{\frac{3}{2}}} + u_z + v_z \tag{22}$$

$$\ddot{r} = r\omega^2 - \frac{\mu}{r^2} \tag{23}$$

$$\dot{\omega} = -\frac{2\dot{r}\omega}{r} \tag{24}$$

where x, y, and z are the radial, in-track, and cross-track rectangular coordinates of the maneuvering spacecraft relative to the target spacecraft; u_x, u_y, and u_z are the control accelerations of the maneuvering spacecraft; v_x, v_y, and v_z are the process noise terms that represent model uncertainty; r and ω are the radius and the angular velocity of the target spacecraft; and μ is the gravitational parameter of the central body.

For spacecraft using a radar system for rendezvous navigation, the transformation of variables

$$x = \rho \cos\phi \cos\theta \tag{25}$$

$$y = \rho \cos\phi \sin\theta \tag{26}$$

$$z = \rho \sin\phi \tag{27}$$

has been suggested by Eggleston and Dunning,[17] where ρ is the range between the maneuver spacecraft and the target spacecraft, θ is the azimuth angle, and ϕ is the relative elevation angle. After the substitution of this transformation, the relative motion dynamics are given by

$$\ddot{\boldsymbol{\eta}} = \boldsymbol{f}_a(\boldsymbol{\eta}, \dot{\boldsymbol{\eta}}, t) + \boldsymbol{G}_a(\boldsymbol{\eta})(\boldsymbol{u} + \boldsymbol{v}) \tag{28}$$

where $\boldsymbol{\eta} = \{\rho \;\; \theta \;\; \phi\}^T$, $\boldsymbol{u} = \{u_\rho \;\; u_\theta \;\; u_\phi\}^T$, $\boldsymbol{v} = \{v_\rho \;\; v_\theta \;\; v_\phi\}^T$, $\boldsymbol{f}_a = \{f_\rho \;\; f_\theta \;\; f_\phi\}$, and

$$f_\rho(\boldsymbol{\eta}, \dot{\boldsymbol{\eta}}, t) = (\omega^2 + 2\omega\dot{\theta} + \dot{\theta}^2)\rho\cos^2\phi + \rho\dot{\phi}^2 - \frac{\mu(r\cos\theta\cos\phi + \rho)}{(r^2 + \rho^2 + 2r\rho\cos\theta\cos\phi)^{\frac{3}{2}}} + \frac{\mu}{r^2}\cos\theta\cos\phi \tag{29}$$

$$f_\theta(\boldsymbol{\eta}, \dot{\boldsymbol{\eta}}, t) = 2(\omega + \dot{\theta})\dot{\phi}\tan\phi - \dot{\omega} - 2(\omega + \dot{\theta})\frac{\dot{\rho}}{\rho} + \frac{\mu(r\sin\theta\sec\phi)}{\rho(r^2 + \rho^2 + 2r\rho\cos\theta\cos\phi)^{\frac{3}{2}}} - \frac{\mu}{r^2\rho}\sin\theta\sec\phi \tag{30}$$

$$f_\phi(\boldsymbol{\eta}, \dot{\boldsymbol{\eta}}, t) = -\frac{1}{2}(\omega + \dot{\theta})^2 - \frac{2\dot{\rho}\dot{\phi}}{\rho} - \frac{\mu}{r^2\rho}\cos\theta\sin\phi + \frac{\mu r\cos\theta\sin\phi}{\rho(r^2 + \rho^2 + 2r\rho\cos\theta\cos\phi)^{\frac{3}{2}}} \tag{31}$$

$$\boldsymbol{G}_a(\boldsymbol{\eta}) = \begin{bmatrix} 1 & 0 & 0 \\ 0 & \dfrac{1}{\rho} & 0 \\ 0 & 0 & \dfrac{1}{\rho} \end{bmatrix} \tag{32}$$

The control and process noise terms are represented in the spherical coordinate system by means of the transformation

$$\begin{Bmatrix} u_\rho \\ u_\theta \\ u_\phi \end{Bmatrix} = \begin{bmatrix} \cos\phi\cos\theta & \cos\phi\sin\theta & \sin\phi \\ -\sin\theta & \cos\theta & 0 \\ -\sin\phi\cos\theta & -\sin\theta\sin\phi & \cos\phi \end{bmatrix} \begin{Bmatrix} u_x \\ u_y \\ u_z \end{Bmatrix} \tag{33}$$

$$\begin{Bmatrix} v_\rho \\ v_\theta \\ v_\phi \end{Bmatrix} = \begin{bmatrix} \cos\phi\cos\theta & \cos\phi\sin\theta & \sin\phi \\ -\sin\theta & \cos\theta & 0 \\ -\sin\phi\cos\theta & -\sin\theta\sin\phi & \cos\phi \end{bmatrix} \begin{Bmatrix} v_x \\ v_y \\ v_z \end{Bmatrix} \tag{34}$$

The overall state vector is then $\boldsymbol{x} = \{\boldsymbol{\eta}^T \;\; \dot{\boldsymbol{\eta}}^T\}^T$. The measurement model in the relative spherical coordinate system is simply

$$\boldsymbol{y}_k = \boldsymbol{H}_k\boldsymbol{x}_k \tag{35}$$

where the measurement matrix is

$$\boldsymbol{H}_k = \begin{bmatrix} 1 & 0 & 0 & 0 & 0 & 0 \\ 0 & 1 & 0 & 0 & 0 & 0 \\ 0 & 0 & 1 & 0 & 0 & 0 \end{bmatrix} \tag{36}$$

Note that the coordinate transformation given by Eqs. (25–27) leads to a linear measurement equation. This simplification of the measurement equation comes at the cost of introducing state-dependant process noise, given by Eq. (34). It is expected from the results in Ref. 18 that the reformulation of the dynamic model into one that gives a linear measurement equation will improve the estimation errors over one in which the measurement equation is nonlinear.

The next section is focused on a simple guidance scheme for the purposes of simulating the Kalman filter and Huber filter during rendezvous scenarios.

Rendezvous Guidance and Control

In this section, the guidance and control required for executing a rendezvous maneuver are discussed. The rendezvous controller is based on a simple feedback linearization, followed by a choice of gains to decouple the range, azimuth, and elevation dynamics. By defining a desired state $\boldsymbol{\eta}_d$ and $\dot{\boldsymbol{\eta}}_d$ and choosing a nonlinear feedback control law of the form

$$\boldsymbol{u}(\boldsymbol{\eta}, \dot{\boldsymbol{\eta}}, t) = -\boldsymbol{G}_a(\boldsymbol{\eta})^{-1}[\boldsymbol{f}_a(\boldsymbol{\eta}, \dot{\boldsymbol{\eta}}, t) + \boldsymbol{K}_p(\boldsymbol{\eta} - \boldsymbol{\eta}_d) + \boldsymbol{K}_d(\dot{\boldsymbol{\eta}} - \dot{\boldsymbol{\eta}}_d)] \tag{37}$$

the closed-loop system becomes

$$\ddot{\boldsymbol{\eta}} + \boldsymbol{K}_d(\dot{\boldsymbol{\eta}} - \dot{\boldsymbol{\eta}}_d) + \boldsymbol{K}_p(\boldsymbol{\eta} - \boldsymbol{\eta}_d) = \boldsymbol{0} \tag{38}$$

The closed-loop system is asymptotically stable for any choice of gain matrices such that $\boldsymbol{K}_p > 0$ and $\boldsymbol{K}_d > 0$. In particular, with $\boldsymbol{K}_p$ and $\boldsymbol{K}_d$ chosen to be diagonal, the closed-loop system is decoupled. A similar control law has been proposed by Kluever in Ref. 19, although the present method is superior in that it is based on the nonlinear (but Keplerian) orbital dynamics rather than the Clohessy–Wiltshire equations[20] and that it also includes the cross-track motion.

The guidance commands originate as follows. In general rendezvous maneuvers there is some required approach direction. The required approach direction can be characterized by a desired azimuth angle θ_d. Likewise, the initiation of the final approach to the target may be characterized by a desired initial range ρ_d. The final approach along the inbound azimuth angle may then have a desired range rate $\dot{\rho}_d$. Thus, the rendezvous maneuver can be divided into two phases. First, the maneuver is made into the required approach direction at the given initiation range. Second, the final approach is made along the incoming azimuth at the desired range rate. The desired state can be then written as $\boldsymbol{\eta}_d = \{\rho_d \;\; \theta_d \;\; 0\}^T$ and $\dot{\boldsymbol{\eta}}_d = \{0 \;\; 0 \;\; 0\}^T$ for the first phase and $\boldsymbol{\eta}_d = \{0 \;\; \theta_d \;\; 0\}^T$ and $\dot{\boldsymbol{\eta}}_d = \{\dot{\rho}_d \;\; 0 \;\; 0\}^T$ for the second phase of the maneuver. The phase of the rendezvous maneuver can be switched when the states in the first phase are within some prescribed tolerance of the desired initial condition for the second phase. This guidance scheme is crude, but adequate for the purpose of demonstrating the performance of the filtering algorithms during rendezvous maneuvers.

Numerical Simulation

In this section, the numerical simulations conducted to demonstrate the improvement in navigation performance to be found by using the Huber filter in place of the Kalman filter is described.

In the sample problems and simulations described in this section, the rendezvous scenario takes place in a low lunar orbit, with a target vehicle with perilune altitude of 100 km and an apolune altitude of 200 km. The initial conditions of the maneuvering vehicle are at the time of perilune passage of the target vehicle and are provided in Table 1. Table 1 shows the true value of the initial conditions, the estimate of the initial conditions for filter initialization, and the components of the initial variance matrix for filter initialization. The initial covariance matrix is assumed to be diagonal. In other words, the initial state errors are uncorrelated.

The initial conditions for the target orbit, desired rendezvous conditions, and other simulation parameters are shown in Table 2. The controller gains are specified in Table 3. The gains are chosen such

Table 1 Initial conditions

Initial state	True value	Estimated value	Standard deviation
$\rho(0)$, km	1.0	1.05	0.01
$\theta(0)$, deg	0.0	0.5	0.1
$\phi(0)$, deg	10.0	10.5	0.1
$\dot{\rho}(0)$, km/s	0.0	5.0×10^{-4}	1.0×10^{-4}
$\dot{\theta}(0)$, deg/s	0.0	5.0×10^{-3}	0.01
$\dot{\phi}(0)$, deg/s	0.0	5.0×10^{-3}	0.01

Table 2 Other initial conditions and parameters

Parameter	Value
$r(0)$, km	1838
$\omega(0)$, deg/s	0.0516
μ, km^3/s^2	4902.87
ρ_d, km	0.1
θ_d, deg	180.0
$\dot{\rho}_d$, km/s	-1.0×10^{-4}
γ	1.345
κ	0.9
$\bar{\omega}$	8.5354×10^{-4}
$E(v_x^2) = E(v_y^2) = E(v_z^2)$, km^2/s^4	10^{-12}

Table 3 Diagonal elements of gain matrices

Gain	Value	Gain	Value
$K_p(1,1)$	$\bar{\omega}^2$	$K_d(1,1)$	$2\kappa\bar{\omega}$
$K_p(2,2)$	$4\bar{\omega}^2$	$K_d(2,2)$	$4\kappa\bar{\omega}$
$K_p(3,3)$	$4\bar{\omega}^2$	$K_d(3,3)$	$4\kappa\bar{\omega}$

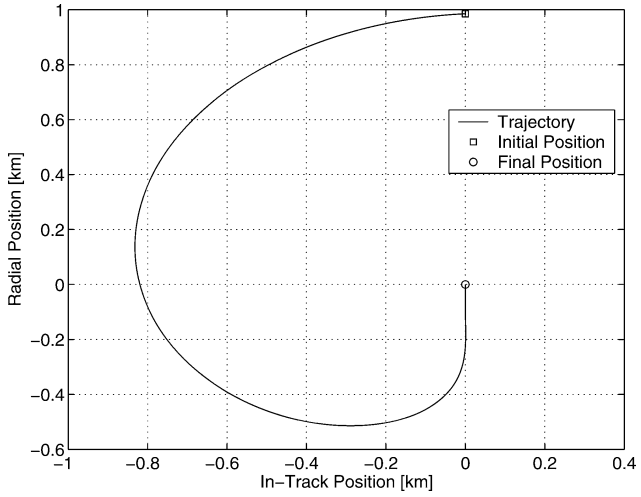

Fig. 1 In-plane projection of nominal maneuver.

that the damping ratio $\kappa = 0.9$ and the natural frequency of the error dynamics $\bar{\omega}$ are equal to the mean motion of the target orbit for the range dynamics and twice the mean motion of the target orbit for the azimuth and elevation dynamics.

The maneuver spacecraft is assumed to make use of a laser navigation sensor to make direct measurements of the range and line of sight to the target spacecraft. The sensor random uncertainties, provided in Table 4, were taken from Ref. 21 as an example of a rendezvous navigation sensor that has recently flown in space and used in a rendezvous scenario.

Random measurement errors are drawn from the mixture of zero-mean Gaussian probability distributions, defined by the probability density function

$$p(\zeta) = \left[(1-\epsilon)/\sigma_1\sqrt{2\pi}\right]\exp\left[-(\zeta/\sigma_1)^2/2\right] + \left(\epsilon/\sigma_2\sqrt{2\pi}\right)\exp\left[-(\zeta/\sigma_2)^2/2\right] \tag{39}$$

where σ_1 and σ_2 are the standard deviations of the individual Gaussian distributions and ϵ is a perturbing parameter that represents error model contamination. For purposes of the rendezvous maneuver simulation, the standard deviations σ_1 are chosen according to Table 4 and σ_2 is chosen as $\sigma_2 = 5\sigma_1$. The measurements are assumed to occur at a frequency of 1 Hz along the trajectory.

An in-plane projection of the nominal maneuver (perfect navigation) is shown in Fig. 1. The time to perform the nominal maneuver is 7233 s (approximately 0.98 periods of the target spacecraft orbit).

The results of a Monte Carlo simulation of the rendezvous maneuver using the Huber filter and the Kalman filter are shown in Fig. 2. The median state estimate error variances from 100 simulation runs are shown as a function of the perturbing parameter ϵ. The Kalman filter results are shown in the dashed curve and the Huber filter results are shown in the solid curve. The Huber filter and Kalman filter are very close to one another for the case $\epsilon = 0$.

Table 4 Rendezvous navigation sensor uncertainties

Measurement	Standard deviation (σ_1)
Range (ρ), cm	1.518
Azimuth (θ), mdeg	2.787
Elevation (ϕ), mdeg	1.404

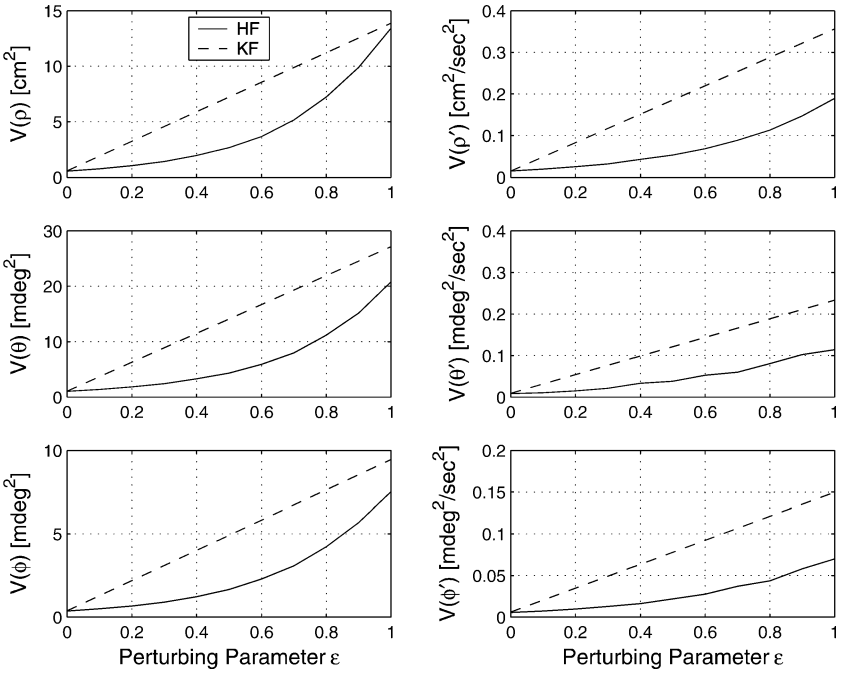

Fig. 2 Monte Carlo results.

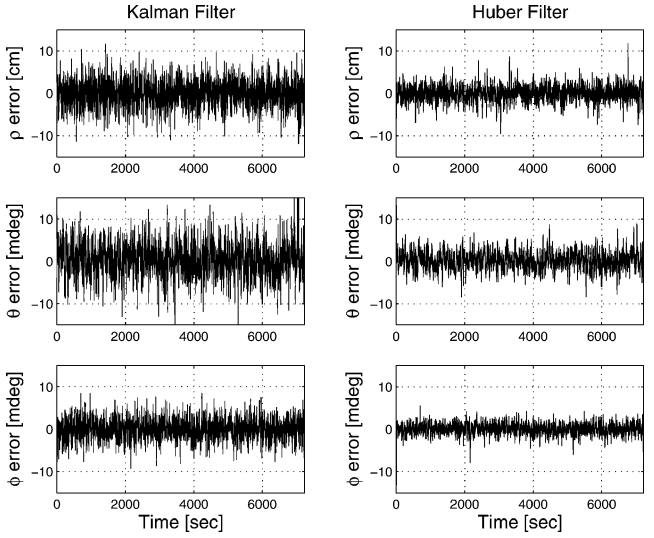

a) Position error

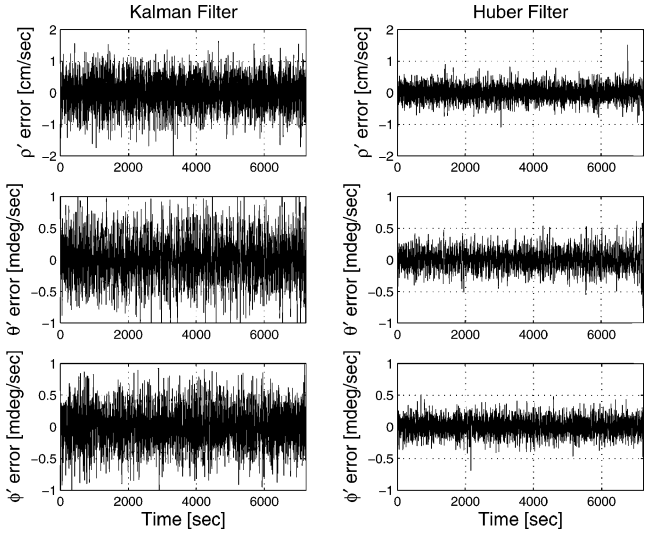

b) Velocity error

Fig. 3 Position and velocity estimation errors during rendezvous maneuver for $\epsilon = 0.5$.

As ϵ increases, however, the Kalman filter variances increase much more rapidly than the Huber filter variances. Note that the rate of divergence of the Kalman filter variances relative to the Huber filter variances as ϵ increases is not gradual. In fact, the variance of the Huber filter estimates remains almost flat, even with as much perturbation as $\epsilon = 0.2$. The shallow nature of the Huber filter results are due to the robustness of the estimation technique to thickly tailed measurement error distributions.

The estimation error time histories are shown in Fig. 3 for the case of $\epsilon = 0.5$. The position estimation errors are shown in Fig. 3a, and the velocity estimation errors are shown in Fig. 3b. In both Figs. 3a and 3b, the Kalman filter estimation error is shown in the left column, and the Huber filter estimation error is shown in the right column. Note that there is no scale change between the Kalman filter results and the Huber filter results and that the Huber filter estimation errors are smaller than the Kalman filter estimation errors.

The improvement in estimation error comes at a cost in computation due to the iterative nature of the measurement update equation. The results of the Monte Carlo study indicate that the increase in overall computation time is roughly 10%, which implies that the Huber filter should still be fast enough for real-time implementation.

Conclusions

In this Note, the application of a robust state estimation method to the problem of relative navigation during spacecraft rendezvous maneuvers in elliptical orbit is discussed. The robust filter is a recursive form of the Huber estimator, which in turn is blend of the least-squares estimation and the least absolute value estimation techniques. This combined technique has a proven robustness with respect to deviations from the common assumption of Gaussian distributed random measurement errors. The robust method was compared with the Kalman filter or recursive least-squares method during a sample rendezvous trajectory, using a perturbed Gaussian distribution as the basis for generating random measurement errors. The results demonstrate that the Huber filter outperforms the Kalman filter for non-Gaussian measurement error probability distributions in terms of the state estimation error variances for a 10% increase in computational burden.

References

[1]Polites, M. E., "Technology of Automated Rendezvous and Capture in Space," *Journal of Spacecraft and Rockets*, Vol. 36, No. 2, 1999, pp. 280–291.

[2]Ruoff, C., "Technologies for Mars Exploration and Sample Return," AIAA Paper 99-4447, Sept. 1999.

[3]Moses, R. W., Van Laak, J., Johnson, S. L., Chytka, T. M., Amundsen, R. M., Dorsey, J. T., Doggett, W. R., Reeves, J. D., Todd, B. K., Stambolian, D. B., and Moe, R. V., "Analysis of In–Space Assembly of Modular Systems," AIAA Paper 2005-2504, Jan. 2005.

[4]Kalman, R. E., "A New Approach to Linear Filtering and Prediction Problems," *Journal of Basic Engineering,* Vol. 82, No. 1, 1960, pp. 35–50.

[5]Tukey, J. W., "A Survey of Sampling from Contaminated Distributions," *Contributions to Probability and Statistics*, edited by I. Olkin, S. Ghurye, W. Hoeffding, W. Madow, and H. Mann, Stanford Univ. Press, Stanford, CA, 1960, pp. 448–485.

[6]Huber, P. J., "Robust Statistics: A Review," *Annals of Mathematical Statistics*, Vol. 43, No. 4, 1972, pp. 1041–1067.

[7]Wu, W. R., "Maximum Likelihood Identification of Glint Noise," *IEEE Transactions on Aerospace and Electronic Systems*, Vol. 32, No. 1, 1996, pp. 41–51.

[8]Junkins, J. L., Akella, M. R., and Alfriend, K. T., "Non-Gaussian Error Propagation in Orbital Mechanics," *Journal of the Astronautical Sciences*, Vol. 44, No. 4, 1996, pp. 541–563.

[9]Huber, P. J., "Robust Estimation of a Location Parameter," *Annals of Mathematical Statistics*, Vol. 35, No. 2, 1964, pp. 73–101.

[10]Huber, P. J., *Robust Statistics*, Wiley, New York, 1981, pp. 43–106.

[11]Duncan, D. B., and Horn, S. D., "Linear Dynamic Recursive Estimation from the Viewpoint of Regression Analysis," *Journal of the American Statistical Association*, Vol. 67, No. 340, 1972, pp. 815–821.

[12]Beaton, A. E., and Tukey, J. W., "The Fitting of Power Series, Meaning Polynomials, Illustrated on Band-Spectroscopic Data," *Technometrics*, Vol. 16, No. 2, 1974, pp. 147–185.

[13]Hampel, F. R., "The Influence Curve and Its Role in Robust Estimation," *Journal of the American Statistical Association*, Vol. 69, No. 346, 1974, pp. 383–393.

[14]Hampel, F. R., Rousseeuw, P. J., Ronchetti, E., and Stahel, W. A., *Robust Statistics: The Approach Based on Influence Functions*, Wiley, New York, 1986, pp. 78–186.

[15]Holland, P. W., and Welsch, R. E., "Robust Regression Using Iteratively Reweighted Least Squares," *Communications in Statistics: Theory and Methods*, Vol. 6, No. 9, 1977, pp. 813–827.

[16]Schaub, H., and Junkins, J. L., *Analytical Mechanics of Space Systems*, AIAA Education Series, AIAA, Reston, VA, 2003, pp. 594–599.

[17]Eggleston, J. M., and Dunning, R. S., "Analytical Evaluation of a Method of Midcourse Guidance for Rendezvous with Earth Satellites," NASA TN D-883, June 1961.

[18]Mohanty, N. C., "Autonomous Navigation for High Altitude Satellites," *Information Sciences*, Vol. 30, No. 2, 1983, pp. 125–150.

[19]Kluever, C. A., "Feedback Control for Spacecraft Rendezvous and Docking," *Journal of Guidance, Control, and Dynamics*, Vol. 22, No. 4, 1999, pp. 609–611.

[20]Clohessy, W. H., and Wiltshire, R. S., "Terminal Guidance System for Satellite Rendezvous," *Journal of the Aerospace Sciences*, Vol. 27, No. 5, 1960, pp. 653–658, 674.

[21]Mokuno, M., Kawano, I., and Suzuki, T., "In-Orbit Demonstration of Rendezvous Laser Radar for Unmanned Autonomous Rendezvous Docking," *IEEE Transactions on Aerospace and Electronic Systems*, Vol. 40, No. 2, 2004, pp. 617–626.